

# Design of the Aluminum Vacuum Chambers for the TPS

G. Y. Hsiung<sup>1</sup>, C. K. Chan<sup>1</sup>, T. L. Yang<sup>1</sup>, C. K. Kuan<sup>1</sup>, C. C. Chang<sup>1</sup>, C. L. Chen<sup>1</sup>, H. P. Hsueh<sup>1</sup>,  
J. R. Chen<sup>1,2</sup>

<sup>1</sup>NSRRC, 101 Hsin-Ann Road, Hsinchu 300, Taiwan

<sup>2</sup>Dept. of Biomedical Engineering & Environmental Sciences, NTHU, Hsinchu 300, Taiwan

## Abstract

*The aluminum bending chambers for the Taiwan Photon Source (TPS) is designed to meet the requirement of ultra high vacuum condition for the electron beam of 3 ~ 3.3 GeV and 400 mA. The crotch absorbers are located far from the source to reduce the synchrotron radiation power density thus the design of the cooling is simple. A program of finite element analysis is applied to simulate the thermal loading near the crotch absorber where the heat load is the highest. Normal incident of the irradiation on the absorbers is possible that the production-yields of photon stimulated desorption as well as the photoelectrons are minimized. The vacuum pumps are mounted closed to the source of outgas major coming from the absorbers and form a localized pumping in the antechamber. The broadband impedance from the beam duct is reduced since the quantity of pumping holes or slots is dramatically reduced. Feasibilities of the design for the TPS Al vacuum chambers will be described.*

## 1. Introduction

The latest lattice design for the Taiwan Photon Source (TPS) has been proposed to meet the requirements of beam energy at 3 to 3.3 GeV, beam current at 400 mA, and the emittance  $< 2$  nm-rad [1]. The electron storage ring, with a circumference of 518.4 m, has 6-fold super period of DBA structure with 24 unit cells in total. The vacuum system for the electron storage ring provides an ideal vacuum environment to ensure the stability of circulated electron beam and continuous emission of stable synchrotron light. Design of the vacuum system for the synchrotron light source considers the maximum power with 3.3 GeV and 500 mA as the upper bound. To ensure the stability of the circulating electron beam, the vacuum system for the storage ring is constructed with consideration of the following factors, (1) Sustaining the ultrahigh vacuum (UHV), (2) Highly stable vacuum system, (3) Vacuum chambers with low impedance, (4) Thermal absorbers, (5) Highly reliable vacuum system. The aluminum alloys (Al) are selected for the vacuum chambers based on the successful experiences of existed 1.5 GeV Taiwan Light Source (TLS) [2,3]. The design concepts are described in the following sections.

## 2. Vacuum Chambers

The basic parameters for the TPS vacuum system are shown in the Table 1. The design concepts for the vacuum system are described in the following sections.

Table 1: Basic Parameters for the TPS

Parameters	Symbols	Values
Beam Energy	$E$	3.0 GeV
Beam Current	$I$	400 mA
Bending Radius of Dipoles	$\rho$	7.2575 m
Bending Angle	$\theta$	7.5 °
Critical Energy	$\varepsilon_c$	8.25 keV

### **2.1. General Design Criteria**

The pressure should be less than 1 nTorr to obtain a beam life time longer than 10 hours. All vacuum vessels and parts must be made from UHV-compatible materials. Vacuum parts must undergo critical surface cleaning to minimize the rate of surface outgassing. The rate of leakage after welding and assembling of vacuum chambers should be  $< 1 \times 10^{-10}$  Torr·L/s. Only oil-free vacuum pumps are used to evacuate the chambers to prevent contamination from the back-streaming of oil. Vacuum gauges with detection range  $< 1 \times 10^{-11}$  Torr are used to read the pressure. The level of vibration for the vacuum chambers, especially near the fixed beam position monitors (BPM), should be  $< 0.1 \mu\text{m}$  with supports. The precision of the manufacture of vacuum chambers and parts should be  $< \pm 0.5$  mm under general conditions, and that of high-precision parts should be  $< \pm 0.1$  mm. The inner cross section of the electron-beam duct should be maintained as smooth as possible. The height of the steps inside the ducts should be  $< 0.5$  mm in general but  $< 0.3$  mm for each beam duct associated with an insertion device (ID) that has a small vertical aperture  $< 20$  mm. For vacuum components, such as flanges, bellows, pumping slots, with a break or discontinuous structure, other RF contact pieces should be installed to shield the gaps in the surface. The change in the cross section of the tapers should be smooth with an angle of inclination  $< 1/10$ . Some interiors of the beam ducts can be machined to give them a saw-tooth structure to decrease the flux of scattered light and the yield of photoelectrons. The photon absorbers must be designed to be suitable for all situations, not only routine operation but also during specific beam adjustments or tuning, that requires particular cooling. Efficient structures to transfer heat are required to prevent potential problems of thermal outgassing or melt-down. The vibration of the cooling pipes of photon absorbers should be decreased to  $< 0.1 \mu\text{m}$  by isolation. All vacuum components installed in the tunnel for the storage ring should be able to withstand, or should be shielded from, radiation in high doses. The status of vacuum gauges, flow meters and thermometers for the chambers, absorbers and water, as well as the protection trigger circuits, are connected to the vacuum interlock system for online monitoring and security controls. The interlock system and the control power supplies for the vacuum pumps and the gauges must be directly connected to the emergency power lines via uninterruptible power supplies (UPS).

### **2.2. Selection of Materials for the Chambers**

For the TLS, aluminum alloys are the basic materials of the beam duct chambers of the electron-storage ring. As the key technologies for machining, cleaning and welding the aluminum-alloy chambers have been well established domestically, the development of various aluminum beam ducts for insertion devices and gas-cell chambers for beam lines has been successful. Besides, the unique characteristics of aluminum alloys with great thermal conductivity, zero residual radioactivity, and other useful properties support their application in synchrotron accelerators. If the TPS continues to use aluminum alloys to make the vacuum chambers, the existing equipment, facilities and technical experience will remain applicable, increasing the efficiency and reliability of the constructed system. Manufacturing technologies will be improved and domestic manufacturers will be able to continue maintenance. The chosen materials used to make the beam ducts of the storage ring are strong aluminum alloys, including A6063T6, A6061T5 and A5083T321, by either extrusion or machining. The flanges for connecting and sealing are made of harder aluminum alloys such as A2219T87. The gasket for sealing is made of a soft A1050 aluminum alloy. The photon absorbers are made of either aluminum alloys or oxygen free high conductive (OFHC) copper, depending on the requirements of the cooling structures and the power densities to which they are subjected.

### **2.3. Structural Design**

The vacuum chambers in the straight sections are of three kinds - long straight (LS), medium straight (MS) and short straight (SS). Six LS sections each of length 11.7 m and 18 MS sections each of length 7 m, in total 24, contain chambers for injection kickers, RF cavities, diagnostics, and insertion devices. The cross section of the beam duct is elliptical with inner diameters 32 mm and 70 mm for accommodating the dynamic apertures. The thickness of aluminum chambers is typically 4 mm. The beam ducts for insertion devices are designed to meet the specifications. The taper chambers invariably accommodate adjacent chambers that have different cross sections.

The vacuum chambers in the bending sections, called B-chambers, are designed to accommodate the spaces among the adjacent magnets of types dipole (D-), quadrupole (Q-) and sextupole (S-). One sextant super-period comprises B-chambers of eight types, B1 ~ B8, so the storage ring has in total 48 B-chambers. Figure 1 presents the assemblies of one unit cell (1/24 of storage ring) of two B-chambers coexisting with the magnets. The B-chamber is designed as a long triangular chamber with an antechamber on the near side of the electron-beam duct. Local photon absorbers are installed inside the antechamber and located near the downstream side. The absorbers are located as far from the light source as practicable to diminish the power density of the heat load. Vacuum pumps with a high pumping speed are located near the photon absorbers to evacuate emitted gas due to photon-stimulated desorption (PSD) and to decrease the amount of gaseous flow back to the beam channel. On the other hand, more spaces are available for locating the pumps in the antechambers rather than in the beam ducts. The open gap between the antechamber and the beam duct is 10 mm high and > 60 mm wide along the beam duct which is enough for photon extraction. Impedance of the beam duct is lower since the quantities of pumping holes, flanges, and bellows, are reduced. The cooling channels to absorb the thermal load from irradiating synchrotron light are made by drilling holes in the chamber walls downstream of the B-chambers. Some flanges are available if more individual absorbers or photon apertures are required to decrease the thermal load. The assembly drawings of B1 chamber and cross section views of B1 chamber with Q- and S-magnets are shown in figure 2. The supports for the chambers are fixed to the ground and isolated from the magnets and girders. Clearance between the chambers and Q-, S-magnets is kept ~ 3 mm for providing enough space of beam based alignment.

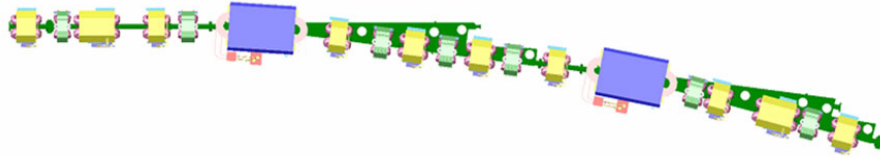


Figure 1. Assembly drawing of one unit cell, 1/24 of storage ring, contains two B-chambers and the magnets.

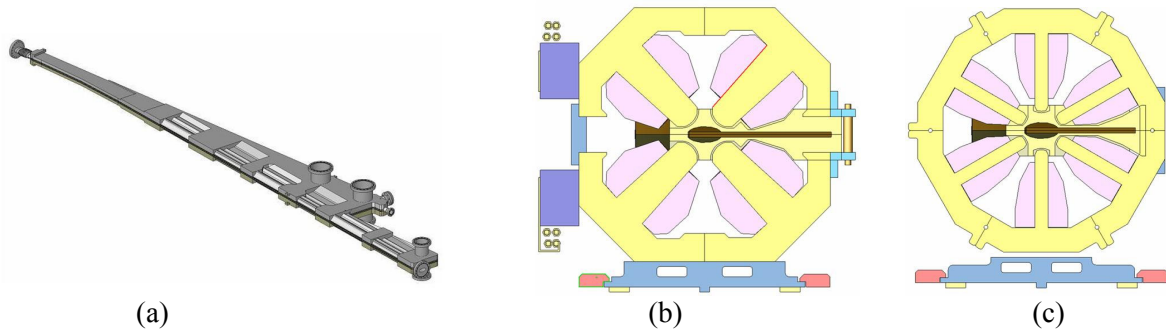


Figure 2. Assembly drawings of (a) B1 chamber, and cross section views of B1 chamber with (b) Q-magnet, and (c) S-magnet.

#### 2.4. Finite Element Analysis

For the large size triangular shape B-chamber about 4 ~ 5 m in length, the backside of one half chamber is machined according to the shapes of poles and coils for the Q- and S- magnets along the beam duct, while the inside is machined the channels for the electron beam and the photon ports. The deformation of the B-chamber due to evacuation is concerned and simulated with the ANSYS program. The result for the B1 chamber, made of A6061T5 Al, is shown in figure 3. The maximum deformation, shown in red color, addresses 0.131 mm near the Q- and S- magnets, but < 0.1 mm in the beam duct.

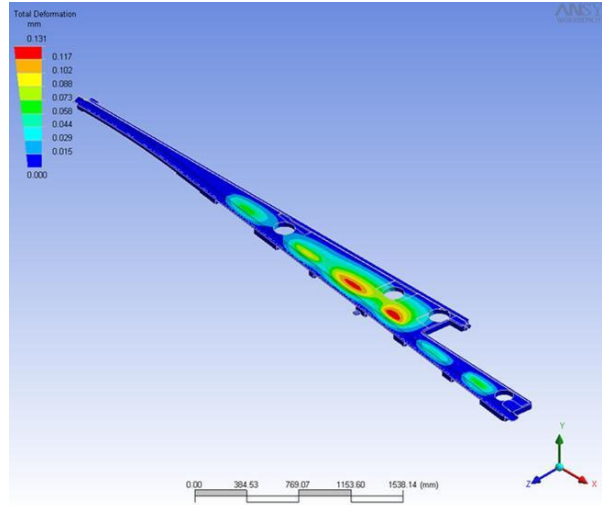


Figure 3. Simulation of the deformation on the lower half of B1 chamber due to the evacuation.

The thermal distribution on the downstream Al absorber with interior drilled cooling channels is simulated by the ANSYS program as well. The result is shown in figure 4. The maximum power density of the synchrotron light, at 3 GeV and 400 mA, irradiated on the surface of absorber located at 3.3 m far is  $22 \text{ W/mm}^2$ . However, the maximum temperature at the hot spot, shown in red color in figure 4, is  $121^\circ\text{C}$  with a saw-tooth structure of 0.4 mm in step-height and 2 mm in width for each step. The result will be a guide for the following design of the absorbers to evaluate the capabilities of taking the synchrotron light at maximum power at 3.3 GeV and 500 mA according the distance from the source.

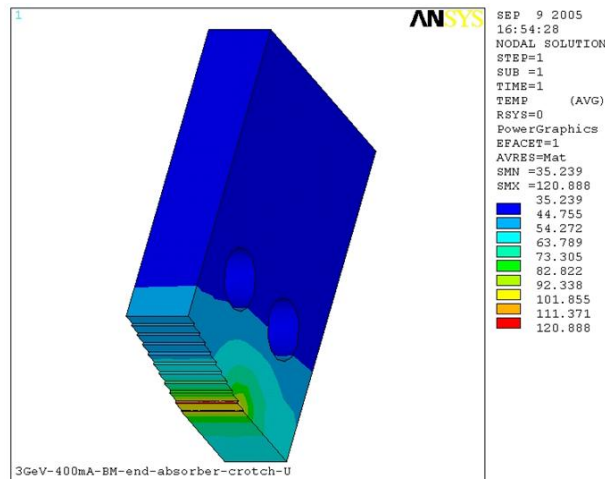


Figure 4. Simulation of the thermal distribution on the downstream Al absorber with interior cooling.

### 3. Manufacturing and Treatment

The manufacturing procedures for aluminum chambers are based on the experiences established for the TLS vacuum systems. The processes contain the machining, cleaning, welding, assembling, testing, evacuation, vacuum baking, and installation, are described as follows.

#### 3.1. Machining

The straight chambers are made by extrusion of aluminum. The bending chambers are divided into two half plates and produced by NC machining with pure alcohol spraying such that the surface after machining is protected from the ambient atmosphere contaminated with oil. The machined pieces are stored and sealed inside an aluminum bag filled with dry nitrogen gas after the machining has been

completed; they are then shipped to the NSRRC. The machined pieces are not removed from the bag before they arrive in a clean room with controlled humidity. All subsequent welding of the two halves of the chambers, including the cooling pipes and the flanges, is performed inside the clean room.

### **3.2. *Cleaning and Welding***

When vacuum chambers or parts have been machined in an environment without cleaning, the fresh surface after machining immediately forms a layer of oxide contaminated with oil. Oil vapors then desorb from the surface during evacuation to reside in the peripheral vacuum system. The surface oxide and oil layers can typically be removed only with stringent chemical cleaning. In the vacuum chamber after machining, the residual machining oil should be cleaned away using strong alkaline detergents, and then rinsed with clean water. The surface-oxide layer is then removed by immersion in strong acid, and rinsed again in clean water. The final step is to rinse the parts in de-ionized water (resistance  $> 10\text{ M}\Omega$ ) with ultrasonic vibration and then to dry them with hot air before transferring them into the clean welding room for welding. The current process for cleaning the aluminum chambers at NSRRC follows a standard procedure developed in CERN; other procedures from various foreign national laboratories are used also to produce an ideal clean surface. The use of some liquids is restricted by environmental-protection policies; such solvents are replaced with other new solutions, which must be approved following the results of experimental testing and surface analysis before use. The aluminum chambers and parts are welded using tungsten-inert-gas (TIG) welding processes. The welding is performed in a clean room of Class  $\sim 1000$ . The relative humidity of the clean room is maintained at  $< 50\%$  during the welding.

### **3.3. *Assembly and Test***

Following welding, the vacuum chambers are inspected using an oil-free vacuum leak detector to discover any leakage from the welded parts. Leakage from the detector at a rate  $> 1 \times 10^{-10}$  Torr L/s can be detected. Leakage from pipes for cooling water is tested by both methods - vacuum leak detection and sniff detection. The welded parts are tested after welding to determine whether a pressure  $10\text{ kg/cm}^2$  is maintained inside the pipes. All assembly tasks of the vacuum systems are undertaken in a clean room of Class 10000 or better, to ensure that the vacuum chamber remains clean and has low micro-dust content. For the assembled vacuum systems, the leakage test is conducted using a vacuum leak detector or a residual gas analyzer (RGA) to ensure that the chambers do not leak before the subsequent vacuum-baking test is performed.

### **3.4. *Evacuation and Baking***

To prevent back-stream oil contamination, only oil-free pumps are used to evacuate the vacuum systems. As all surfaces of a vacuum chamber contain much adsorbed water, evacuating them to an UHV condition is difficult. After absence of leaks has been confirmed, the entire vacuum system should be evacuated and uniformly baked at a temperature  $150\text{ }^\circ\text{C}$  for 24 h to remove outgassing water from surfaces. In the final stage of baking, the sputtering ionization pumps and the gauges should be degassed and the non-evaporable getter (NEG) pump should be activated before cooling. The vacuum leak test should be performed at room temperature after baking. Only SIP and NEG pumps are used to maintain the long-term UHV condition. Because the spaces between the vacuum chambers and the magnets or other parts in the tunnels are too tight to wrap the heaters, Al foil and Kapton insulating sheets reserved for baking, pre-baking to UHV of a entire unit cell of the vacuum system in the laboratory is planned, sealing it with gate valves before transport to the tunnel and subsequent alignment. No baking occurs inside the tunnel. Baking on site for chambers supplied with hot water at high pressure might be considered, rather than wrapping the heaters. The fixed points on the chambers will be adjusted to their original positions with a tolerance  $< 50\text{ }\mu\text{m}$ .

### **3.5. *Installation and alignment***

During the machining of the vacuum chambers, the base planes for alignment purposes should be defined. Some holes on the base planes are drilled for the fiducial targets those are used in the subsequent installation and alignment on site. To ensure the precise alignment of the overall system of the storage ring, the design of the vacuum chambers and the schemes of alignment should be approved

by the members of the mechanical-positioning group. Two-sector gate valves will be installed on both sides of each unit cell, which contains two bending chambers, to simplify the alignment and adjustment of the vacuum chambers in the bending sections. A set of jigs and fixtures is designed for the chambers in each complete cell to support the overall assembly, and a baking test is performed to verify the ideal vacuum conditions in the clean room, transfer to the storage-ring tunnel, hanging by a crane, and mounting on girders and supports. The work required to evacuate and to perform baking inside the tunnel can be diminished, and the alignment work simplified. The precision of alignment of the vacuum chamber is  $\pm 0.5$  mm in general, and  $\pm 0.1$  mm for special parts.

#### 4. Pumping Configurations

For the electron storage ring, two major outgassing sources are from thermal desorption and PSD. Two computer codes are employed to simulate the pressure profiles of the TPS vacuum systems. One is called "iteration method" as the one dimensional simulation for the straight sections, the other is called "Monte Carlo method" as the two dimensional simulation for the bending sections.

##### 4.1. Iterative method

The iterative method utilizes the continuity principle of the gas law [4]. It is useful for the vacuum systems with a simple structure such as the straight sections. Two simulations on the pressure distribution have been done for the long straight sections containing the long flat beam ducts for the undulator and many kinds of discrete chambers for the injection and diagnostic elements, as shown in figure 5(a) and (b). The pumps of NEG strips with speed of 3 L/s·cm are considered in the straight sections for the undulator, while the types of lumped NEG or the SIP with speed of 400 L/s are selected in the injection section. The averaged pressure obtained at  $\eta = 5 \times 10^{-5}$  molecules/electron is 0.12 nTorr for LS-undulator, and 0.11 nTorr for LS-Injection.

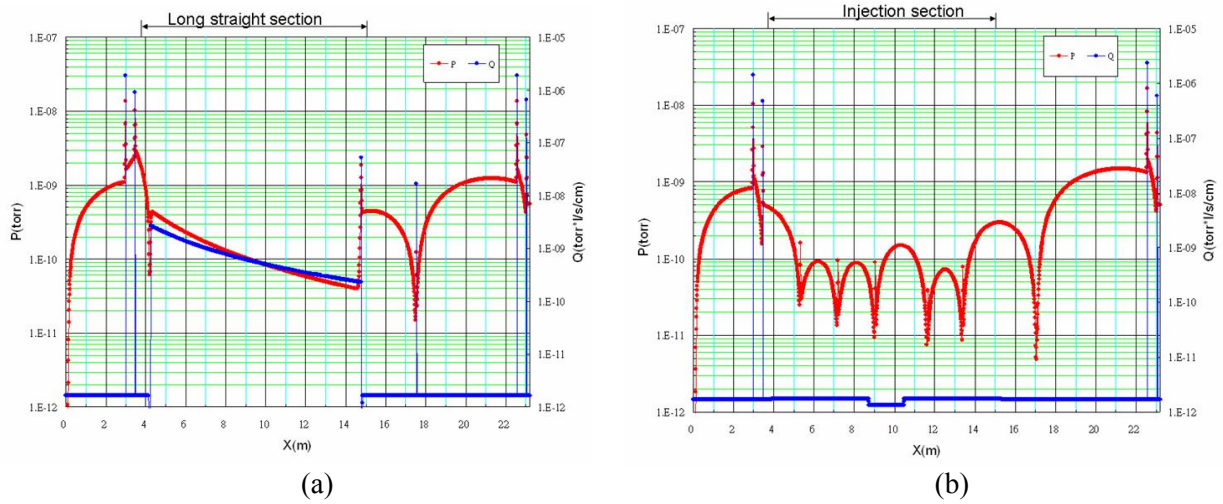


Figure 5. Pressure profiles for the long straight section (a), and the injection section (b).

##### 4.2. Monte Carlo method

The Monte Carlo method is more suitable than the iterative method for a vacuum system with complex conductance, such as the bending chambers. The approach employed herein can calculate the time evolution of the pressure profile by tracing sample particles at various times [5]. For triangular-like B-chambers, photon absorbers are installed inside the antechamber at a distance 3 ~ 4 m from the source, and subjected to irradiated power at a small density. The absorber can thus absorb this radiation from the synchrotron light at normal incidence, at which the  $\eta$ -value is least. Figure 6 presents the pressure profile of a B-chamber installed three 400 L/s vacuum pumps, obtained by the Monte Carlo method, at a desorption coefficient of  $\eta = 1 \times 10^{-5}$  molecules/electron. The maximum pressure is 1.9 nTorr and the average pressure can reach a value  $< 1.0$  nTorr.



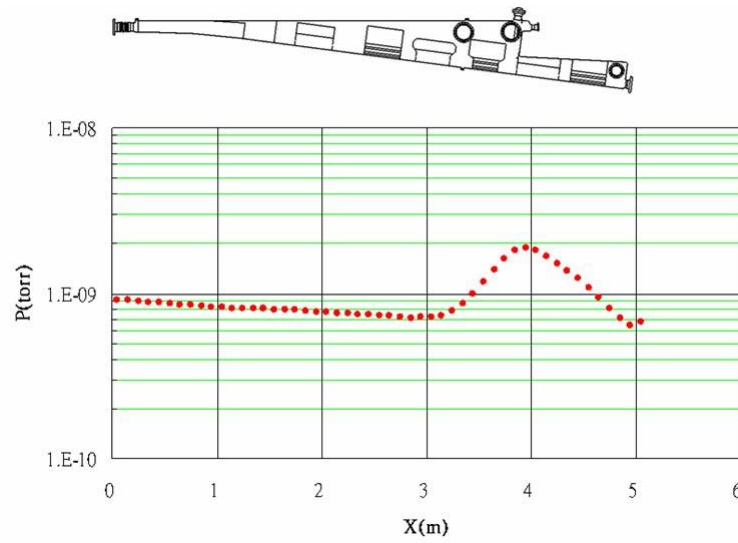


Figure 6. Pressure profile for one of the B-chambers.

## 5. Front Ends

The front ends for the insertion devices (ID-FE) are designed according to the kinds of light source. The maximum peak power density to be taken in case of 3 GeV, 400 mA, will be  $33 \text{ kW/mr}^2$  for an elliptical polarized undulator (EPU46), or  $170 \text{ kW/mr}^2$  for a superconducting undulator (SU15) [1]. Besides, a maximum total power to be taken will be 62 kW in case of the superconducting wiggler (SW60) [1]. The high heat load components for the ID-FE should be carefully designed for taking such high power loads. However, the front ends for the bending magnet source (BM-FE) can be designed to a standard type. Since all the heat load components as well as the chambers are located downstream the aluminum B-chambers. Thus all the vacuum chambers including the absorbers or masks can be made of aluminum alloys. Figure 7 illustrates the assembly drawing of a BM-FE which contains two sets of photon beam position monitors (PBPM), photon absorber (PAB), heavy metal shutter (HMS), NEG and IP pumps, and the main chamber. The main chamber, made of Al, is manufactured by the way similar to that for the Al bending chambers. A simple NC machining work on the inner surfaces of two halves is done prior to the TIG welding in the humidity-controlled clean room. The pre-mask will be machined inside the chamber between the first IP and PBPM1, which is not shown in Figure 7, providing an entrance aperture for the transmitted photon beam. The cooling channels for the mask will be drilled through the bulk of chamber closed to the mask. Supporting for the PBPM assemblies is isolated with the vacuum chamber by the bellows and fixed to the ground.

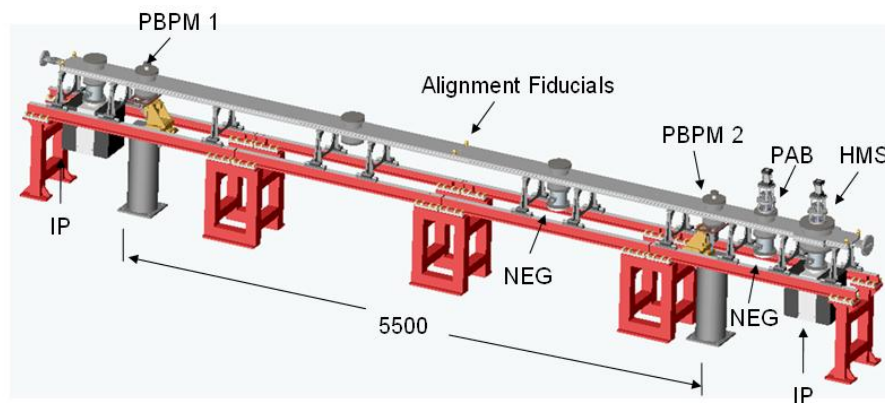


Figure 7. Assembly drawing of a front end for the bending magnet source. The symbols in the figure represent the PBPM for photon beam position monitor, PAB for photon absorber, HMS for heavy metal shutter, and the Alignment Fiducials for the align targets.

## 6. Conclusions

Conceptual design for the 3 GeV TPS vacuum systems made of aluminum alloys is evaluated. The large size B-chambers contain several benefits including the reduction of impedance for the beam duct, high efficient local pumping structures, localized absorbers far from the source, and simplest interior structure in the part of antechamber. Similar concept is applied to the BM-front ends. Design for the absorbers in some of B-chamber is to be improved for reduction of the surface temperature.

## 7. References

- [1] C.C. Kuo, H.P. Chang, G.H. Luo, H.J. Tsai, M.H. Wang, and C.T. Chen, Proceedings of 2005 Particle Accelerator Conference, Knoxville, Tennessee, 2005, p. 2989.
- [2] J.R. Chen, J.C. Chang, L.H. Chang, C.T. Chen, F.Z. Hsiao, K.T. Hsu, G.Y. Hsiung, C.S. Hwang, C.C. Kuo, W.K. Lau, K.K. Lin, K.B. Liu, G.H. Luo, Ch. Wang, and D.J. Wang, Proceedings of APAC 2004, Gyeongju, Korea, 2004, p. 510.
- [3] G.Y. Hsiung, S.N. Hsu, T.F. Lin, K.M. Hsiao, C.C. Chang, C.K. Chan, J.Y. Yang, K.Y. Kao, and J.R. Chen, Proceedings of APAC 2004, Gyeongju, Korea, 2004, p. 640.
- [4] D.C. Chen, G.Y. Hsiung, and J. R. Chen, J. Vac. Soc. R.O.C (1), (1987) 24.
- [5] Y. Suetsugu, J. Vac. Sci. Technol. A14(1), (1996) 245.